

Research Reports

A new method for detection and quantification of heart-beat parameters in *Drosophila*, zebrafish, and embryonic mouse hearts

Martin Fink^{1,2}, Carles Callol-Massot^{3,4}, Angela Chu¹, Pilar Ruiz-Lozano⁵, Juan Carlos Izpisua Belmonte^{4,6}, Wayne Giles^{1,7}, Rolf Bodmer⁵, and Karen Ocorr⁵

¹Department of Bioengineering, University of California, San Diego, La Jolla, CA, USA, ²Cardiac Electrophysiology Group, Department of Physiology, Anatomy and Genetics, Oxford University, Oxford, England, ³Scientific Department, Biobide, San Sebastian, Gipuzkoa, Spain, ⁴Gene Expression Laboratory, Salk Institute for Biological Studies, La Jolla, California, USA, ⁵Development and Aging Program, Neuroscience, Aging, and Stem Cell Research Center, Burnham Institute for Medical Research, La Jolla, CA, USA, ⁶Center of Regenerative Medicine in Barcelona, Barcelona, Spain, and ⁷the Faculty of Kinesiology, University of Calgary, Calgary, Alberta, Canada

BioTechniques 46:101-113 (February 2009) doi 10.2144/000113078

Supplementary material for this article is available at www.BioTechniques.com.

The genetic basis of heart development is remarkably conserved from *Drosophila* to mammals, and insights from flies have greatly informed our understanding of vertebrate heart development. Recent evidence suggests that many aspects of heart function are also conserved and the genes involved in heart development also play roles in adult heart function. We have developed a *Drosophila* heart preparation and movement analysis algorithm that allows quantification of functional parameters. Our methodology combines high-speed optical recording of beating hearts with a robust, semi-automated analysis to accurately detect and quantify, on a beat-to-beat basis, not only heart rate but also diastolic and systolic intervals, systolic and diastolic diameters, percent fractional shortening, contraction wave velocity, and cardiac arrhythmicity. Here, we present a detailed analysis of hearts from adult *Drosophila*, 2–3-day-old zebrafish larva, and 8-day-old mouse embryos, indicating that our methodology is potentially applicable to an array of biological models. We detect progressive age-related changes in fly hearts as well as subtle but distinct cardiac deficits in *Tbx5* heterozygote mutant zebrafish. Our methodology for quantifying cardiac function in these genetically tractable model systems should provide valuable insights into the genetics of heart function.

Introduction

The fruit fly, *Drosophila*, is a powerful genetic model system with a multitude of tools for manipulating genes and gene expression. This system has provided valuable insight into the cellular mechanism underlying heart development in the fly and this information has led to the identification of key regulators of heart development in vertebrates. Several groups have begun to examine heart function in the fruit fly with the goal of using this system as a physiological model that can be manipulated genetically (1–8). Genetic manipulations of ion channel genes in *Drosophila*, including L-type Ca²⁺ channels and several types of K⁺ channels, suggest that the currents

contributing to heart function in flies are remarkably similar to those in human hearts (3,8–11). Several mutations produce effects in the fly that mimic human heart disease syndromes (3,5) reviewed in References 12–14. Thus, the fly heart will be useful as a myocardial model of human heart disease.

A number of methods have been developed to detect and quantify heart rate in fruit flies. Manual counting of heart beats visualized through the cuticle of intact pupae and flies has been used previously, but is not practical or accurate for long periods of time or during periods of high-frequency beating. Heart rates have also been obtained by manual counting from slow motion replay of videotape recordings (2), which provides a more

accurate determination of rate but does not provide information about the relative lengths of diastole and systole, which are important parameters for detailed heart beat analysis. Automated detection of light intensity changes has also been used to provide an objective measure of heart rate (10,11,15–21), as has edge tracing (6), but again, these methods primarily provide information about rate. Electrical recordings (22) can also be used to provide heart rate information, but obtaining stable recordings from beating hearts is technically difficult even for short periods of time. Finally, optical coherence tomography (OCT) (7) has been employed to obtain a number of heart beat parameters, including diastolic and systolic intervals, but this method requires highly

specialized equipment, tracks heart activity for only limited periods of time, has limited spatial resolution, and requires manual calculations of a limited numbers of beats from M-mode records. Thus, it is desirable to standardize and automate a method for obtaining reliable measurements of the dynamic parameters of heart function for large samples of individuals over significant periods of time and for all the heart beats in a record.

We have developed a methodology for analyzing a number of contraction-relaxation parameters in the myogenic heart of *Drosophila* that is also applicable to other model systems. Our method combines a denervated, exposed fly heart with a unique set of movement detection algorithms that automatically and precisely detect and measure beat-to-beat contraction parameters captured in low or high speed movies providing both analytical and statistical power. The output provides detailed information concerning pacemaker activity and contraction-relaxation parameters including heart rate, systolic intervals (SI) and diastolic intervals (DI), systolic and diastolic diameters, contraction strength, heart rhythmicity, and contraction wave velocity (CWV) along the heart tube. We have successfully used these movement detection algorithms to quantify heart beat parameters in *Drosophila*, as well as larval zebrafish and embryonic mouse hearts.

Materials and methods

Semi-intact *Drosophila* heart preparation

Two wild-type laboratory strains of *Drosophila* (yw and w^{1118}) were maintained and aged as described previously (3,6). Abdominal heart tubes were exposed by cutting off the head and ventral thorax of the fly and then removing the ventral abdominal cuticle and all internal organs. Dissections were performed under an artificial adult hemolymph (based on References 23 and 24) containing 108 mM NaCl₂, 5 mM KCl, 2 mM CaCl₂, 8 mM MgCl₂, 1 mM NaH₂PO₄, 4 mM NaHCO₃, 15 mM 4-(2-hydroxyethyl)-1-piperazineethanesulfonic acid (HEPES), 10 mM sucrose, and 5 mM trehalose, at pH 7.1. Recordings of heart activity were acquired from semi-intact *Drosophila* preparations at room temperature using a Hamamatsu EM-CCD digital camera (McBain Instruments, Chatsworth, CA, USA) mounted on a Leica DM-LFSA microscope with a 10× water immersion lens (McBain Instruments) and Simple PCI image capture software (Compix

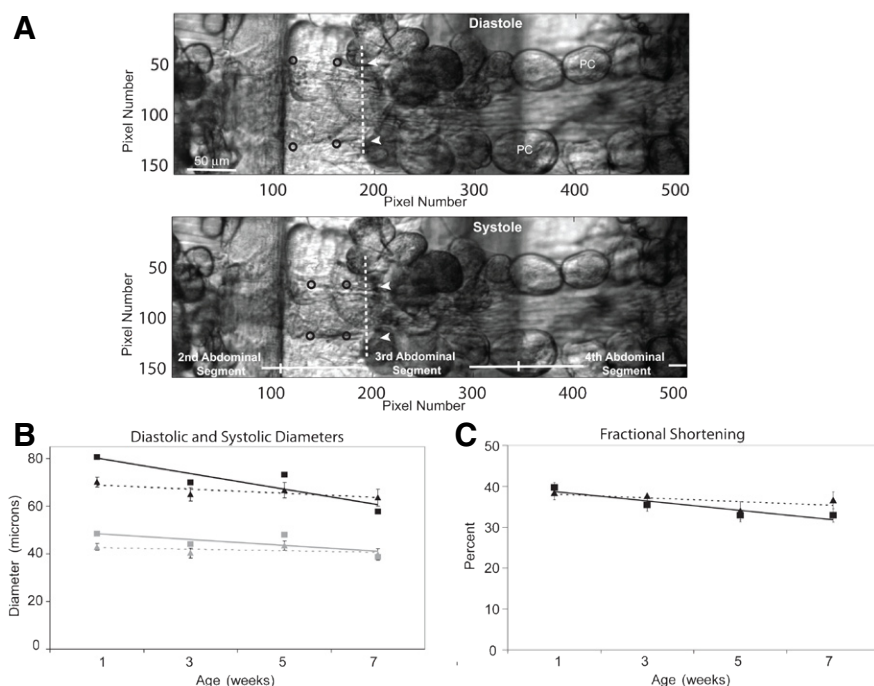


Figure 1. Systolic and diastolic heart diameters. (A) Movie still of three segments in the fly abdomen showing the exposed heart during diastole. The position of the heart walls is indicated by white arrowheads, and circles indicate positions marked by the user and used by the program to calculate heart diameters. The vertical dashed lines show the orientation of pixel strips used to generate the M-modes shown in Figure 2. (B) The same fly heart during systole; arrowheads mark the changed location of the heart tube edge during contraction. (C) Quantification of the diastolic and systolic diameter measurements for yw and w^{1118} laboratory wild-type strains of *Drosophila*. Data points represent the mean (\pm SEM) for 17–30 flies per data point. The decrease in diastolic diameter shows a significant age dependence (ANCOVA, $P = 0.003$) but the systolic diameter decrease is not significant in this study (ANCOVA, $P = 0.08$). (square, yw strain; triangle, w^{1118} strain). Black lines represent diastole, gray lines represent systole. (D) Percent fractional shortening (% FS) provides an estimate of the ejection volume and is obtained from the data shown in C (see Equation 2). The decrease of % FS with age is significant (ANCOVA, $P = 0.04$) and is due to the relatively greater decrease of diastolic diameter as compared to systolic diameter. (square, yw strain; triangle, w^{1118} strain).

Imaging System, Selwicky, PA, USA). Frame rates were 100–150 fps; all movies were 60 s in length. See Supplementary Movie 1 (available at www.BioTechniques.com) for an example.

Detection and quantification of movement due to heart contractions

We use a combination of two movement detection algorithms written in Matlab (The MathWorks, Inc., Natick, MA, USA) to accurately track movement of the heart edges. The first approach, the Frame Brightness Algorithm, tracks changes in average light intensity of each frame. This approach has been employed previously using lower-speed devices (2,10,15,18,21) to detect and quantify heart rate in *Drosophila*. The second approach, the Changing Pixel Intensity Algorithm, detects movement by comparing the intensity changes in individual pixels from one frame to the next. Our program also tracks heart movements by creating an M-mode, similar to techniques used previously for analyzing human echocar-

diograms (25). A summary is available in Supplementary Algorithm Details, available at www.BioTechniques.com.

Frame Brightness Algorithm

For our semi-intact *Drosophila* heart preparation, frame brightness decreases during the contractions, because as the heart muscle cells contract the contractile proteins and cell membranes become more concentrated and obscure more of the transmitted light (compare Figure 1, A with B). The mean brightness value of all the pixels in a frame is calculated for every frame in the movie (Figure 2, A and B), similar to (15). Low-frequency oscillations in the signal due to fluctuations in background illumination can be removed later using a high-pass filter (see Supplementary Figure 1, available at www.BioTechniques.com).

Changing Pixel Intensity Algorithm

During heart contractions, the darker pixels, corresponding to the edges of the heart tube, move over the lighter

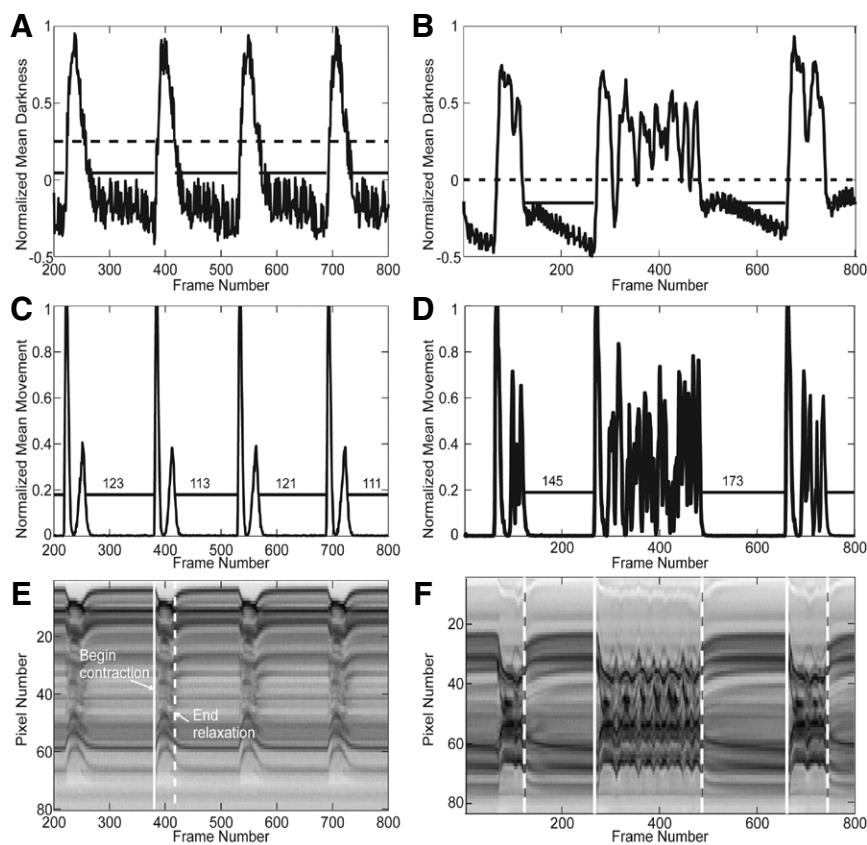


Figure 2. Movement detection from high-speed digital movies. (A) Movement detection for a 1-week-old fly using the Frame Brightness Algorithm; peaks indicate individual heart contractions. (B) Movement detection for a 1-week-old fly using the Changing Pixel Intensity Algorithm. For each beat the first peak represents the movement due to contraction, whereas the second (or additional) movement is due to relaxation. The number of frames for each detected diastolic interval is printed above the horizontal line which represents the movement threshold. (C) M-mode generated by electronically excising and aligning 1-pixel-wide, vertical strips from successive movie frames. These strips span the heart tube and are taken from the same location in each frame of the movie (approximately the middle of the third abdominal segment; see dashed lines in Figure 1, A and B). Thus, M-modes show movement of the heart tube edges (in the vertical y-axis) over time (on the x-axis). The movie frames analyzed in A and B were used to produce the M-modes shown in C (note alignment of movie frame numbers on the x-axis for panels A–C and D–F); 200 frames represents ~1.5 s. (D) Movement detection using the Frame Brightness Algorithm for a 7-week-old fly. (E) Movement detection using the Changing Pixel Intensity Algorithm for a 7-week-old fly, note incomplete relaxations/non-sustained fibrillations. (Solid line represents the movement threshold and detected diastolic intervals.) (F) M-mode from the same 7-week-old fly movie.

background pixels. Movement can be detected reliably by locating areas where there are significant brightness changes between consecutive movie frames. To determine the areas in the movie that are “moving” between frames, we first calculate the relative brightness change (RBC) for each pixel value (p) in a frame ($f + 1$) relative to the previous frame (f):

$$\text{RBC} = \frac{|p_{f+1} - p_f|}{p_f + 1} \quad [\text{Eq. 1}]$$

The maximum RBC in each frame represents either the movement of a part of the darker membrane over

bright background or, in the absence of movement, the background noise (the minimum value of all the maximum RBCs in a movie). A pixel is considered to be “changing” or “moving” from one frame to the other if the RBC for that pixel is larger than the background noise. The number of changing pixels per frame is normalized to the interval [0, 1] to get comparable results for each movie (Figure 2, C and D). We can display all the “changing” or “moving” pixels in red to illustrate the output of this algorithm (see Supplementary Movie 2, a 1/4 speed version of Supplementary Movie 1, available at www.BioTechniques.com). This algorithm is sensitive enough to discriminate a biphasic movement signal due to both

the contraction and the relaxation movements with minimal noise.

Quantification of heart rate, DI, and SI

A first estimate of the timing and length of diastole is derived by setting a movement threshold (MT) for the Changing Pixels Intensity Algorithm (Figure 2, C and D; Supplementary Figure 1B). The pause in movement occurring during relaxation (diastole) is the DI, the heart period (HP) is quantified as the time between the ends of two consecutive DIs, and SI is quantified as the HP minus the DI. When contractions are relatively prolonged, the algorithm does not always correctly identify the pause during contraction (i.e., an interval with no movement) as part of the SI (Supplementary Figure 1A). In this case, information from the Frame Brightness Algorithm can be used to inform the Changing Pixel Intensity Algorithm as to what state the heart is in (i.e., contracted versus relaxed; compare Supplementary Figure 1, compare A with C). In addition, an upper threshold (blue lines, Supplementary Figure 1) can be set such that movie frame sequences with a darkness level higher than the threshold will not be designated as a pause between contractions or diastolic interval. A second brightness limit can also be set (green lines, Supplementary Figure 1, compare D with E) that ignores movie frame sequences that have a mean darkness level below this threshold even though the darkness levels may be changing. This filters out noise.

To ensure that the detected movement agrees with the contraction events in the movie, the actual movements of the heart tube edges (M-mode trace) are displayed below the movement traces (Supplementary Figure 1 and in-text Figure 2, E and F). M-modes are made by electronically selecting a single vertical row of pixels that spans the heart tube in one frame of the movie and then electronically cutting out the same strip of pixels from every movie frame. These strips are then aligned horizontally, providing an image of the vertical movement of the heart tube edges (y-axis) over time (x-axis). Brief user input is required to verify that the output of the two movement detection algorithms corresponds to the actual contraction pattern shown in the M-mode and to adjust the MT and filters if needed (vertical white lines in Figure 2, E and F). It should be noted that the user input needed to adjust the thresholds and filters potentially introduces inter-operator variability, especially with naive users. However, by using M-mode as an

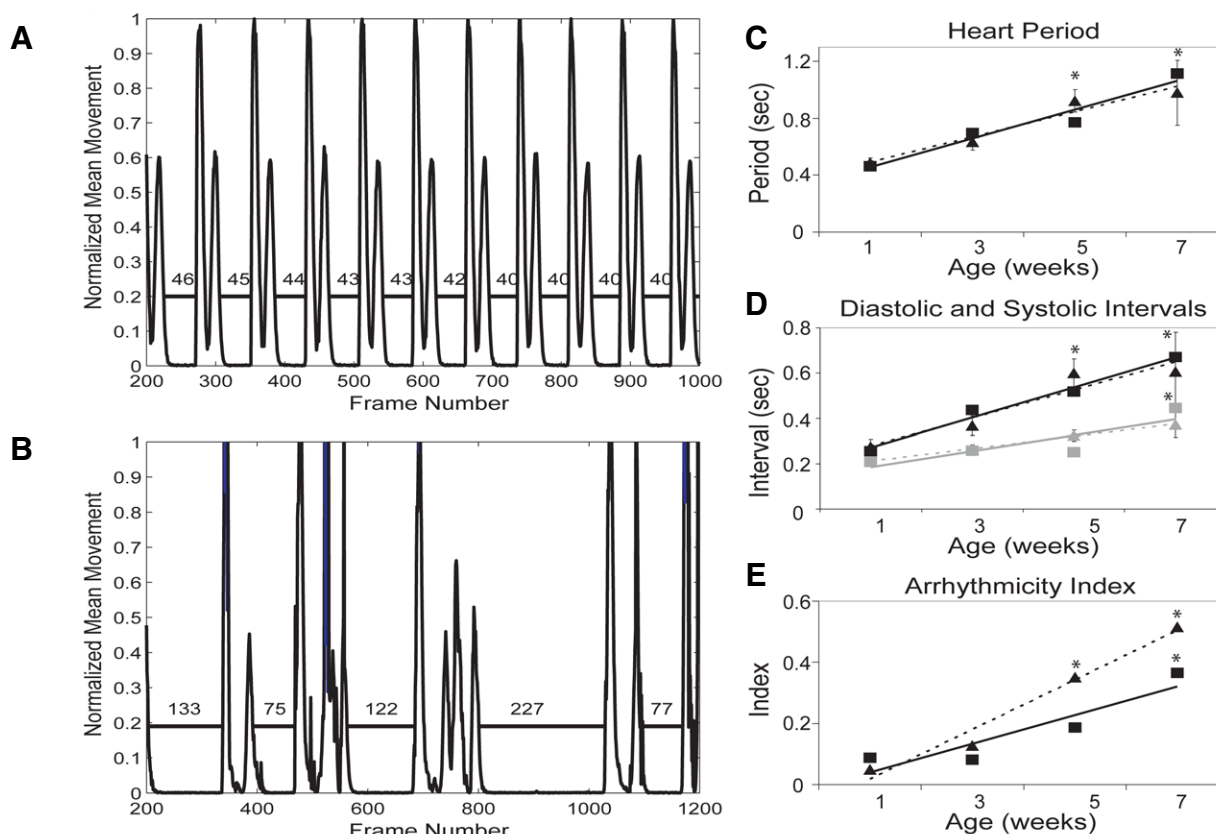


Figure 3. Heart beat intervals and quantification of arrhythmicity. (A) Movement trace showing DI detection (horizontal lines between movement peaks). Duration of the DI is given as the number of frames between successive movement traces; note the regularity of DI in this young (1-week-old) fly. (B) Movement trace from an old fly (5 weeks) showing increased irregularity of both systolic and diastolic interval lengths. (C) Changes in heart period with age (Mean \pm SEM, 17–30 flies per data point). (D) Diastolic intervals (black lines) and systolic intervals (gray lines) showed significant increases as a function of age (Mean \pm SEM, 17–30 flies/data point). (E) “Arrhythmicity Index” (AI) calculated as the heart period standard deviation normalized to the median heart period. Data points represent the average AI for all the flies in each age group (17–30 flies per data point). The age-dependent increase in AI is significant and reflects the observed increase in arrhythmic events that occurs as flies age (shown qualitatively in Figure 2C). For C–E, age-dependent changes in cardiac parameters were modeled hierarchically using ANCOVA, ANOVA for genotype as a function of each parameter and the *t*-tests were employed to determine if there were significant differences between yw and *w¹¹¹⁸* and between young (1-week-old) and old flies [3–7 weeks, **P* < 0.05; see also (3)]. Square, yw strain; triangle, *w¹¹¹⁸* strain.

independent and objective assessment of heart wall movements, to which the algorithm output is finely tuned, this potential for error is greatly diminished. In addition, because the contraction waveforms from the Changing Pixel Intensity Algorithm are usually very sharply defined (for example, Figures 2 and 3, and Supplementary Figure 1), small adjustments of thresholds typically result in only minor fluctuations in the output statistics (see Supplementary Figure 1 legend). If SI and DI detection based on the algorithms differs from the contraction pattern shown by the M-mode, the data are rejected; this occurs in less than 5% of the movies (not shown). Data from each movie is provided in a comma-separated value file.

We can also compare the distribution of HP, DI, and SI data for the total data set. Due to the variability in overall heart rate

between individuals, data are normalized so that the median HP for each record matches up (see Supplementary Figure 2A, available at www.BioTechniques.com). We are also able to quantify the velocity and direction of the contraction wave itself (see Supplementary Figure 3 and Supplementary Algorithm Details, available at www.BioTechniques.com).

Estimates for rhythmicity and abnormal heart contractions

As flies age the HP, DI, and SI lengthen and become more variable; in addition many mutations produce irregular heart rhythms [Figure 3, A and B, (14)]. We used two approaches to quantify these arrhythmicities. One method depends on an estimation of the number of “long” DIs and SIs (Supplementary Figure 2B). Because heart beat parameters are very reproducible for different wild-type

strains at different ages we set specific time intervals for detecting very long or very short heart beat intervals. DIs longer than one second were considered prolonged (bradycardia); this value is approximately 3 times the length of the average DI in regularly beating hearts from young flies (Supplementary Table 1, Figure 3D, available at www.BioTechniques.com). Similarly, we detect unsustainable fibrillation/tachyarrhythmia as the number of SIs that were unusually long (>0.5 s), indicative of sustained contractions. This threshold is twice the average SI, a parameter that showed very little variability in young wild-type flies (Figure 3D). We also include long SIs that were interrupted by very short DIs (<0.06 s, indicative of incomplete relaxations) in this measure.

With age, the HP becomes increasingly more variable and we noted that

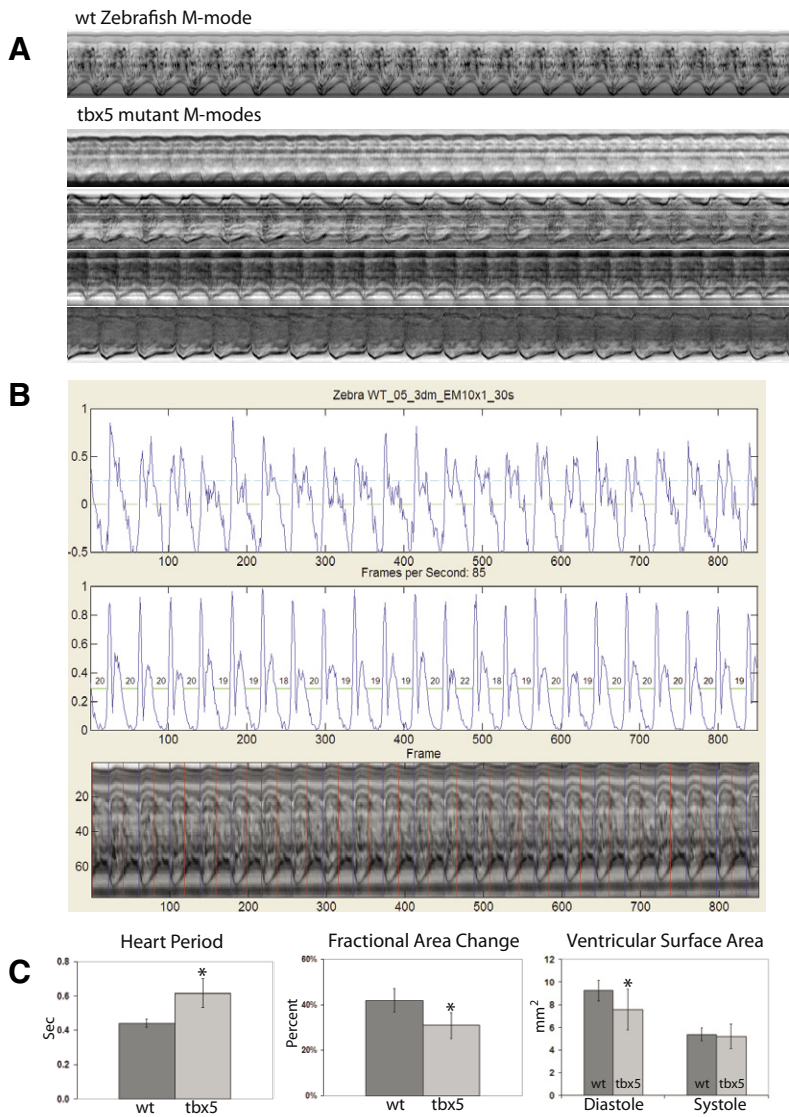


Figure 4. – Zebrafish heart parameters. (A) 10-s M-modes from movies of 2–3-day-old zebrafish hearts. Wild-type M-modes (top trace) show regular heart contractions as evidenced by the significant movement of the heart edge in the dorsal region of the heart (bottom edge trace in the m-mode). All *Tbx5* heterozygotes (lower traces) showed aberrations in their M-modes, primarily characterized by more prolonged contractions with heart wall movements that were noticeably less robust and less fluid. (B) Contraction traces and corresponding M-mode from a wild-type zebrafish showing the correlation between the Changing Pixel Intensity Algorithm and the movements of the heart wall. (C) Heart period was measured as the interval between the start of one diastole and the beginning of the next. Heart periods were measured for every beat in each movie and averaged for each fish. Results for 16 wild-type and 27 *Tbx5* heterozygote zebrafish show a significant increase in the heart period in heterozygotes compared with controls ($*P = 7 \times 10^{-5}$). (D) Percent fractional area change (% FAC) was measured as the percent change in the ventricular surface area between diastole and systole. Heart measurements were made only if all heart edges were clearly visible in the movie frames. Results from 15 wild-type and 12 *Tbx5* heterozygotes show a significant reduction in the % FAC in heterozygotes compared with controls ($*P = 0.02$). (E) A comparison of the ventricular surface areas of hearts measured in (D) during diastole and systole indicate that the decrease in % FAC is due to a decrease in the diastolic size of the hearts. Diastolic surface area of *Tbx5* heterozygotes was significantly smaller than controls whereas systolic surface area did not differ significantly between the two groups ($*P = 0.009$). For C–E, results are given as mean \pm SD. * indicates difference is significant based on unpaired, two-tailed *t*-test.

this is reflected in an increase in the heart period standard deviation measurements for each fly. Thus, we used this standard deviation as an indicator of arrhythmicity in individual flies. We normalized this value to the median HP

in order to compensate for variability between flies and for effects on periodicity due to prolonged contractions. Since the median value is less affected by extreme values (outliers) than the mean, it provides a more accurate representation

of a “normal” HP value. This normalized HP standard deviation we refer to as the arrhythmia index (AI; Figure 3E).

Measurement of heart diameter

In intact flies, the edges of the heart tube are typically obscured by both the pigmented cuticle and abdominal fat bodies. However, in the semi-intact preparation, where some fat cells can be removed, the heart tube edges are usually visible in the third abdominal segment. Markers corresponding to the upper and lower edges of the heart tube can be placed in single movie frames directly on the heart edge (Figure 1, A and B). Movies of beating hearts can be advanced manually to identify frames where maximal contraction and relaxation occur; given average frame rates of 130 fps, this determination is extremely accurate. Because the heart tube is one cell-layer thick, it is usually not possible to resolve an inner and an outer edge. Diastolic and systolic diameters obtained are used to calculate a percent fractional shortening (% FS):

$$\% \text{ FS} = \frac{\text{Diastolic diameter} - \text{Systolic diameter}}{\text{Diastolic diameter}} \times 100, \quad [\text{Eq. 2}]$$

which provides an estimate of the contractility of the heart tube. This calculation assumes that the heart tube dimensions are relatively uniform along its length, which is generally the case for the heart in abdominal segments 3 and 4. It should be emphasized these marks are only used to measure diameters and are not used in the heart movement analysis described in the following sections.

Results

Drosophila semi-intact preparation

As in vertebrates, the fly has a myogenic heart and it resembles the early embryonic human heart in that it is a linear tube with 4 chambers. While it is possible to record movements in the anterior-most portion of the heart (i.e., conical chamber) in intact flies, M-modes prepared from these movies illustrate the complexity of these heart beat patterns as well as the limitations due to image resolution (Supplementary Figure 4, A and B, available at www.BioTechniques.com). As previously reported (4), input from the nervous system alters the heart rate and overall level of contractility (Supplementary Figure 4A). Removing the head (containing cerebral and subesophageal ganglia) appears to have little effect on

the M-mode patterns (Supplementary Figure 4B), but removing the thoracic ventral nerve cord results in a more regular pattern (Supplementary Figure 4C) reminiscent of the patterns seen in the denervated semi-intact preparation (Figure 4C).

The semi-intact preparation functions well in situ for hours following dissection. Heart parameters such as HP, DI, SI, heart diameters, and % FS show a remarkable similarity between flies, and all remain extremely stable for ≥ 4 h, even in preparations from relatively elderly (4-week-old) flies, when supplied with oxygenated, trehalose-supplemented artificial hemolymph (Supplementary Figure 4, D–I). Since recordings are typically performed 30–60 min following dissection, the data generated by our optical method reflects the stable functioning of a myogenic heart tube.

Measurements of heart diameters and fractional shortening

Diastolic and systolic diameters represent the relaxed and contracted state of the heart tube, respectively. Values for these parameters are relatively constant for a

given location throughout the recording period but they will vary according to the region of the heart. For example, the anterior conical chamber region has a larger diameter that narrows dramatically. The posterior portion of the heart is more tubular; consequently, measurements were always made in the same location in abdominal segment 3, which is a relatively linear region of the heart tube (Figure 1A). The average diameters are remarkably similar for both strains of wild-type flies and the measurements appear to be sensitive enough to document small, statistically significant decreases in size for both wild-type strains with age (Figure 1C).

Measurements of heart tube size in both contracted and relaxed states were used to generate an estimate of the volume of hemolymph ejected per longitudinal unit and, indirectly, the strength of the contraction. Ventricular fractional shortening calculated from two-dimensional (2-D) echocardiograms has previously been used as a non-invasive method to assess cardiac function; decreases in this measure are an indicator of reduced contractility and cardiac dysfunction

(26,27) The percent fractional shortening in fly hearts declines slightly but significantly with age suggesting a decline in muscle contractility (Figure 1D and Supplementary Table 1).

Contraction parameters

HP increases significantly with age in wild-type flies (Figure 3C and Supplementary Table 1), consistent with previous observations (2,3). In addition, we are able to document that this increase is due to a disproportionate increase in the DI with age compared with the SI (Figure 3D and Supplementary Table 1). With age, the heart beat patterns also become more disorganized and include periods of fibrillation/tachycardia and asystole/bradycardia, reflected by an increased number of sustained systoles and prolonged diastoles (Figure 2). Detecting prolonged contractions and relaxations as a method to quantify arrhythmia works well when flies are young and the level of arrhythmia is relatively low, but it underestimates arrhythmia in older flies (Supplementary Figure 1B). Because of this, we also use an alternative measure, the AI, which is based on the variability

BrightLine® Fluorescence Filters

Highest Performance. Five Year Warranty. Extensive Inventory.



For fluorescence, Raman and laser systems, ion-beam sputtered optical filters by Semrock are the standard in performance and value.

Semrock®

Visit www.semrock.com/freecatalog
to request a full-color catalog.

of the individual heart periods in a single record. The average AI also exhibits a significant increase with age (Figure 3E) that reflects the age-related increase in arrhythmicity seen in M-mode traces (see Figure 2, E and F).

Fly hearts are able to switch the direction of the contraction wave due to the development of a second pacemaker in the anterior end of the abdominal heart during metamorphosis (4). Our algorithms are able to automatically detect and quantify the direction of contraction during individual beats (Supplementary Figure 3A). This information is provided as a percent of the total beats detected in a record (Supplementary Table 1) and provides an indication of relative function of anterior and posterior pacemakers.

To check the accuracy of the interval detection algorithm, we randomly selected 10 movies of 3-week-old flies and compared manual measurements with the output of our algorithm. Manual measurements for DI and SI were obtained using M-modes in which three representative diastolic and systolic intervals were measured and averaged for each fly. Interval lengths were calculated as the number of pixels (1 pixel = 1 movie frame) divided by the movie speed in frames per second (fps). The results we obtained were similar to those generated by our program for both DI (manual = 0.43 ± 0.07 s, automated = 0.40 ± 0.07 s, mean \pm SEM) and SI (manual = 0.24 ± 0.05 s, automatic = 0.29 ± 0.04 s, mean \pm SEM).

General applicability

Our motion detection algorithms are also applicable to the analysis of movies from two additional model systems: the zebrafish and the mouse.

Larval zebrafish hearts. Zebrafish hearts, like those of *Drosophila* and humans, start out as a linear heart tube and start to loop 24–36 h post fertilization (hpf). We examined hearts between 48–72 hpf, at which point a distinct ventricle and atrium are present (28). Because they are transparent at this stage, heart contractions can be filmed from intact, immobilized larva. Ventricular contractions proved the easiest to analyze (see Supplementary Movie 3, available at www.BioTechniques.com). Movies were taken with anterior to the left of the field and dorsal on the bottom; in this position the ventricle is quite prominent and the program typically tracks the more exaggerated movement exhibited by the dorsal portion of the ventricle.

M-mode records generated by our algorithm show that contractions of the

wild-type larval heart (Figure 4A) have a slightly different shape compared with those in flies (DI is significantly reduced; compare with Figure 2E). As for the fly heart, movement traces generated from zebrafish movies show both contraction and relaxation peaks, but because the program denotes the longer intervals as DI, the labeling of diastole and systole had to be reversed (compare Figure 4B with Figure 2). A comparison of M-mode records indicates that hearts from *Tbx5* heterozygotes contract more slowly and for more prolonged periods than do hearts from wild-type controls (Figure 4, A and B). Indeed, output from our algorithm documents a significant increase in the heart period (reduction in heart rate) in *Tbx5* heterozygotes compared with controls (Figure 4C) due primarily to a significant prolongation of the systolic interval (0.29 ± 0.11 and 0.18 ± 0.05 s, respectively, mean \pm SD, $P = 0.004$) and a smaller but still significant prolongation of the diastolic interval (0.33 ± 0.9 and 0.26 ± 0.11 s, respectively, mean \pm SD, $P = 0.02$).

We can obtain a percent fractional area change (% FAC) measurement by calculating the ventricular surface area using the equation for the area of an ellipse:

$$\frac{a}{2} \times \frac{b}{2} \times \pi, \quad [\text{Eq. 3}]$$

where a is the vertical and b is the horizontal dimension of hearts measured in both diastole and systole (Supplementary Figure 5, A and B, available at www.BioTechniques.com). This is similar to transverse fractional area measurements obtained from vertebrate echocardiograms which show correlations between reductions in fractional area and cardiac dysfunction (27). % FAC is significantly reduced in *Tbx5* heterozygotes (Figure 4D), indicating that cardiac output and contractility is compromised in *Tbx5* heterozygotes, even at very early stages of development. This reduction in contractility appears to be primarily the result of a selective reduction in the diastolic volume in *Tbx5* heterozygotes hearts relative to wild-type (Figure 4E). This conclusion is also supported by the zebrafish M-mode data showing reduced ventricular contraction movements (Figure 4A).

Embryonic mouse hearts. We analyzed hearts from 7.5–8 d mouse embryos (methods in Supplementary Figure 6 legend, available at www.BioTechniques.com); recordings were made from the left side of whole embryos prior to looping while the heart tube is still relatively linear (Supplementary Movie 4, available at www.BioTechniques.com). Heart tube contractions at this stage are easily tracked by the Changing Pixel Intensity Algorithm (Supplementary Figure 6) and resemble the contraction/relaxation patterns seen in flies. The output from our analysis showed an average heart rate of 1.4 ± 0.12 Hz (mean \pm SD), which is within the 1–2 Hz range of rates typically obtained for 8.5 d embryos using visual observation (29) or Doppler analysis (30). In addition, our analysis permitted a determination of the relative DI (0.41 ± 0.04 s, mean \pm SD) and SI (0.32 ± 0.03 s, mean \pm SD).

Discussion

We have developed a novel methodology for movement detection in high speed movies and for quantification of a number of heart beat parameters. Previous methods in intact flies or pupae have been primarily limited to the quantification of heart rate (2,4,6,7,9,10,15,16,18–21,31,32). In addition, interpretation of data obtained from hearts in vivo is confounded by the contribution of nervous input to heart contraction patterns, rate, and overall dimensions (4,20) (see also Supplementary Figure 4, A–C). The semi-intact preparation we have developed allows us to selectively examine the function of cardiomyocytes in situ in a stably functioning, myogenic heart (Supplementary Figure 4, D–I).

Discussion

Accurate quantification of parameters other than heart rate does not appear to be possible using our Frame Brightness Algorithm or other methods that rely on detection of overall light intensity changes alone. However, using the Changing Pixel Intensity Algorithm we can detect, with great accuracy, both the onset of contraction and the end of relaxation providing precise measurements of DIs and SIs. This is because changes in individual pixel intensities from one movie frame to the next are used to detect movement rather than averaged intensity changes for the entire frame, providing improved sensitivity with very little noise. Equally important is the combined use of output from the Changing Pixel Intensity Algorithm and information from the Frame Brightness Algorithm. This comparison is used because movement detection by the Changing Pixel

Intensity Algorithm is so sensitive that sometimes we detect the contraction and relaxation movements as separate peaks (Figure 2C and Figure 3, A and B). Consequently, when a contraction is sustained for a long period of time (e.g., in older flies), the pause during systole is prolonged and can be interpreted as diastole by the Changing Pixel Intensity Algorithm. The less-sensitive Frame Brightness Algorithm does not detect this pause and therefore can be used to determine whether the heart is contracted (i.e., a peak in darkness is occurring) or is relaxed (i.e., there is no darkness peak). This combinatorial approach results in correct discrimination between the movement pauses occurring during both contraction and relaxation, while permitting an accurate determination of DI, SI, and thus heart rate, on a beat-by-beat basis throughout a large amount of data (Figure 3 and Supplementary Table 1).

Using this system we document age-related changes in fly heart function at a level of detail that provides insight into the physiological basis for these changes. For example, previous studies have shown that heart rate (the inverse of HP) decreases with age in *Drosophila* (2,33) and our data confirms these results (Figure 3C). However, our methodology does more than measure heart rate; the current analysis shows that the age-dependent decrease in heart rate is disproportionately due to increases in the DI (Figure 3D). We also document age-dependent decreases in the fractional shortening or output of the heart (Figure 1, C and D).

The current algorithm also quantifies a more elusive characteristic, the degree of heart beat arrhythmicity. A visual examination of the movies and M-modes provides a qualitative picture of the “arrhythmicity” for individual flies [compare Figure 2, E and F; see also (3)]. However, these results are difficult to express quantitatively and are not useful for comparing groups of individuals. The normalized standard deviation of the HP (“Arrhythmicity Index,” AI), quantifies the variability in the HP for each fly. The AI shows a significant increase with age in flies (Figure 3E) but because this method is not limited to just detecting “long” diastoles or systoles it is likely to be a more flexible and accurate method for generally quantifying arrhythmias.

Interestingly, the age-dependent alterations in heart function that we observe in flies have correlates in humans. Age-dependent decreases in the intrinsic heart rate (34,35) and increases in the incidence of heart arrhythmias have also

been documented in humans (36,37). More recently, KCNQ, a K⁺ channel involved in repolarization in the vertebrate heart, has been shown to be crucial for repolarization of the fly heart (3). Mutations in this channel are known to produce Torsades des Points arrhythmias in human hearts (38) and similar arrhythmic events are seen in KCNQ mutant fly hearts (reviewed in Reference 14). The preparation described here will allow us to describe the cellular and molecular events underlying cardiac function and arrhythmia, document age and gene-related alterations in *Drosophila* heart function, and will be suitable for screening the effects of exogenously applied drugs and other cardioactive agents.

We have quantified parameters in both mouse embryos and larval zebrafish hearts using the same methodology as for flies. Previous studies have successfully used imaging methods to study heart function in zebrafish, but these methods have limitations similar to those discussed above for the fly, in that they provide information only on heart rate (39,40) or require very specialized equipment (41). Nevertheless, studies relying on visual quantification of heart rate have documented bradycardia in zebrafish larva that are homozygous for mutations in the *Tbx5* gene [77% reduction at 48 hpf (39)]. Using our methodology, we have been able to demonstrate significant reductions (20% reduction) in heart rate of similarly aged zebrafish *Tbx5* heterozygotes compared with controls (Figure 4C). The milder effect seen for heterozygotes in the current study is consistent with dosage effects of the *Tbx5* gene previously observed in mouse (42,43). In addition, we were able to document a reduction in % FAC in *Tbx5* heterozygotes that is due to a reduction in the end diastolic diameter, consistent with a recent report of significant reductions in the end diastolic diameters in the adult mouse heart, and altered diastolic function and ventricular stiffness in young humans, both heterozygous for *Tbx5* (44).

Our system for monitoring heart function will allow us to take advantage of the powerful genetic tools that are already available in *Drosophila* to elucidate the genetics underlying cardiac function and cardiac aging. In addition, this system will also be useful for quantifying heart function in at least two other models, the mouse and zebrafish.

Acknowledgements

We are grateful for the financial assistance from the Office of the Deans of

Medicine and Engineering at University of California, San Diego, which provided the Visitor Fellowship to M.F. This study was supported by the National Heart, Lung and Blood Institute (NHLBI; grant nos. R01 HL054732 and R01 HL08949) and the National Institute on Aging (NIA; grant no. P01 AG15434) of the National Institutes of Health (NIH), to R.B.; and the Canadian Institutes of Health Research, the Heart Stroke Foundation of Canada, and an Alberta Heritage Foundation for Medical Research (AHFMR) Medical Scientist Award, to W.G. The financial assistance of the Research Chair of the Heart and Stroke Foundation of Alberta and the N.W.T. is gratefully acknowledged. This study was also supported by funds from the Torres Quevedo and Ikertu program, to C.C.-M.; Fundacion Cellex, the G. Harold and Leila Y. Mathers Charitable Foundation, and MICINN (Ministerio de Innovacion y Ciencia; grant no. BFU-2006-12247) to J.C.I.-B.; and by the Heart and Lung foundation and the National Institutes of Health (NIH; grant no. 1 R01 HL05484, to P.R.-L.). This paper is subject to the NIH Public Access Policy.

The authors declare no competing interests.

References

1. Robbins, J., R. Aggarwal, R. Nichols, and G. Gibson. 1999. Genetic variation affecting heart rate in *Drosophila melanogaster*. *Genet. Res.* 74:121-128.
2. Paternostro, G., C. Vignola, D.U. Bartsch, J.H. Omens, A.D. McColloch, and J.C. Reed. 2001. Age-associated cardiac dysfunction in *Drosophila melanogaster*. *Circ. Res.* 88:1053-1058.
3. Ocorr, K., N. Reeves, R. Wessells, M. Fink, H.S. Chen, T. Akasaka, S. Yasuda, J.M. Metzger, et al. 2007a. KCNQ potassium channel mutations cause cardiac arrhythmias in *Drosophila* that mimic the effects of aging. *Proc. Natl. Acad. Sci. USA* 104:3943-3948.
4. Dulcis, D. and R.B. Levine. 2005. Glutamatergic innervation of the heart initiates retrograde contractions in adult *Drosophila melanogaster*. *J. Neurosci.* 25:271-280.
5. Cammarato, A., C.M. Dambacher, A.F. Knowles, W.A. Kronert, R. Bodmer, K. Ocorr, and S.I. Bernstein. 2007. Myosin transducer mutations differentially affect motor function, myofibril structure, and the performance of skeletal and cardiac muscles. *Mol. Biol. Cell* 19:553-562.
6. Wessells, R.J. and R. Bodmer. 2004. Screening assays for heart function mutants in *Drosophila*. *Biotechniques* 37:58-60.
7. Wolf, M.J., H. Amrein, J.A. Izatt, M.A. Choma, M.C. Reedy, and H.A. Rockman. 2006. *Drosophila* as a model for the identification of genes causing adult human heart

- disease. *Proc. Natl. Acad. Sci. USA* 103:1394-1399.
8. Akasaka, T., S. Klinedinst, K. Ocorr, E.L. Bustamante, S. Kim, and R. Bodmer. 2006. The ATP-sensitive potassium (K_{ATP}) channel-encoded *dSUR* gene is required for *Drosophila* heart function and is regulated by *tinman*. *Proc. Natl. Acad. Sci. USA* 103:11999-12004.
 9. Dowse, H., J. Ringo, J. Power, E. Johnson, K. Kenney, and L. White. 1995. A congenital heart defect in *Drosophila* caused by an action-potential mutation. *J. Neurogenet.* 10:153-168.
 10. Johnson, E., J. Ringo, and H. Dowse. 1997. Modulation of *Drosophila* heartbeat by neurotransmitters. *J. Comp. Physiol. [B]* 167:89-97.
 11. Ray, V.M. and H.B. Dowse. 2005. Mutations in and deletions of the Ca^{2+} channel-encoding gene cacophony, which affect courtship song in *Drosophila*, have novel effects on heartbeating. *J. Neurogenet.* 19:39-56.
 12. Bodmer, R., R. Wessells, E.C. Johnson, and H. Dowse. 2005. Heart Development and Function p.199-250. In Gilbert, L., K., Latraut, and S. Gill (Eds.), *Comprehensive Insect Science*, Elsevier, Amsterdam.
 13. Ocorr, K., N. Reeves, R. Wessells, M. Fink, V. Chen, W. Giles, J. Posakony, and R. Bodmer. 2006. "Cardiac Arrhythmias in the *Drosophila* Model." Symposium Title: Linking Structural Biology to Gene Defects. Keystone Symposia Poster Abstract.
 14. Ocorr, K., L. Perrin, H.-Y. Lim, L. Qian, X. Wu, and R. Bodmer. 2007b. Genetic control of heart function and aging in *Drosophila*. *Trends Cardiovasc. Med.* 17:177-182.
 15. White, L.A., J.M. Ringo, and H.B. Dowse. 1992. Effects of deuterium oxide and temperature on heart rate in *Drosophila melanogaster*. *J. Comp. Physiol. [B]* 162:278-283.
 16. Zornik, E., K. Paisley, and R. Nichols. 1999. Neural transmitters and a peptide modulate *Drosophila* heart rate. *Peptides* 20:45-51.
 17. Zornik, N., A. Duty, and G. Gibson. 2004. Effects of population structure and sex on association between serotonin receptors and *Drosophila* heart rate. *Genetics* 168:1963-1974.
 18. Ashton, K., A.P. Wagoner, R. Carrillo, and G. Gibson. 2001. Quantitative trait loci for the monoamine-related traits heart rate and headless behavior in *Drosophila melanogaster*. *Genetics* 157:283-294.
 19. Dasari, S. and R.L. Cooper. 2006. Direct influence of serotonin on the larval heart of *Drosophila melanogaster*. *J. Comp. Physiol. [B]* 176:349-357.
 20. Wasserthal, L.T. 2007. *Drosophila* flies combine periodic heartbeat reversal with a circulation in the anterior body mediated by a newly discovered anterior pair of ostial valves and 'venous' channels. *J. Exp. Biol.* 210:3707-3719.
 21. Sanyal, S., T. Jennings, H. Dowse, and M. Ramaswami. 2006. Conditional mutations in SERCA, the Sarco-endoplasmic reticulum $Ca(2+)$ -ATPase, alter heart rate and rhythmicity in *Drosophila*. *J. Comp. Physiol. [B]* 176:253-263.
 22. Papaefthmiou, C. and G. Theophilidis. 2001. An in vitro method for recording the electrical activity of the isolated heart of the adult *Drosophila melanogaster*. *In Vitro Cell. Dev. Biol. Anim.* 37:445-449.
 23. Wang, J.W., A.M. Wong, J. Flores, L.B. Vosshall, and R. Axel. 2003. Two-photon calcium imaging reveals an odor-evoked map of activity in the fly brain. *Cell* 112:271-282.
 24. Singleton, K. and R.I. Woodruff. 1994. The osmolarity of adult *Drosophila* hemolymph and its effect on oocyte-nurse cell electrical polarity. *Dev. Biol.* 161:154-167.
 25. Gowda, R.M., I.A. Khan, B.C. Vasavada, T.J. Sacchi, and R. Patel. 2004. History of the evolution of echocardiography. *Int. J. Cardiol.* 97:1-6.
 26. Collins, K.A., C.E. Korcarz, M. Roberto, and R.M. Lang. 2003. Use of echocardiography for the phenotypic assessment of genetically altered mice. *Physiol. Genomics* 13:227-239.
 27. Anavekar, N.S., D. Gerson, H. Skali, R.Y. Kwong, E.K. Yucel, and S.D. Solomon. 2007. Two-dimensional assessment of right ventricular function: an echocardiographic-MRI correlative study. *Echocardiography* 24:452-456.
 28. Stainier, D.Y.R., R.K. Lee, and M.C. Fishman. 1993. Cardiovascular development in the zebrafish. *Development* 119:31-40.
 29. Porter, G.A., Jr. and S.A. Rivkees. 2001. Ontogeny of humoral heart rate regulation in the embryonic mouse. *Am. J. Physiol. Regul. Integr. Comp. Physiol.* 281:R401-R407.
 30. Ji, R.P., C.K. Phoon, O. Aristizabal, K.E. McGrath, J. Palis, and D.H. Turnbull. 2003. Onset of cardiac function during early mouse embryogenesis coincides with entry of primitive erythroblasts into the embryo proper. *Circ. Res.* 92:133-135.
 31. Gu, G.G. and S. Singh. 1995. Pharmacological analysis of heartbeat in *Drosophila*. *J. Neurobiol.* 28:269-280.
 32. Johnson, E., T. Sherry, J. Ringo, and H. Dowse. 2002. Modulation of the cardiac pacemaker of *Drosophila*: cellular mechanisms. *J. Comp. Physiol. [B]* 172:227-236.
 33. Wessells, R.J., E. Fitzgerald, J.R. Cypser, M. Tatar, and R. Bodmer. 2004. Insulin regulation of heart function in aging fruit flies. *Nat. Genet.* 36:1275-1281.
 34. Jose, A.D. and D. Collison. 1970. The normal range and determinants of the intrinsic heart rate in man. *Cardiovasc. Res.* 4:160-167.
 35. Strobel, J.S., A.E. Epstein, R.C. Bourge, J.K. Kirklin, and G.N. Kay. 1999. Nonpharmacologic validation of the intrinsic heart rate in cardiac transplant recipients. *J. Interv. Card. Electrophysiol.* 3:15-18.
 36. Thom, T., N. Haase, W. Rosamond, V.J. Howard, J. Rumsfeld, T. Manolio, Z.J. Zheng, K. Flegal, et al. 2006. Heart disease and stroke statistics--2006 update: a report from the American Heart Association Statistics Committee and Stroke Statistics Subcommittee. *Circulation* 113:e85-e151.
 37. Furberg, C.D., B.M. Psaty, T.A. Manolio, J.M. Gardin, V.E. Smith, and P.M. Rautoharju. 1994. Prevalence of atrial fibrillation in elderly subjects (the Cardiovascular Health Study). *Am. J. Cardiol.* 74:236-241.
 38. Roden, D.M. 2004. Human genomics and its impact on arrhythmias. *Trends Cardiovasc. Med.* 14:112-116.
 39. Garrity, D.M., S. Childs, and M.C. Fishman. 2002. The heartstrings mutation in zebrafish causes heart/fin Tbx5 deficiency syndrome. *Development* 129:4635-4645.
 40. Burns, C.G., D.J. Milan, E.J. Grande, W. Rottbauer, C.A. MacRae, and M.C. Fishman. 2005. High-throughput assay for small molecules that modulate zebrafish embryonic heart rate. *Nat. Chem. Biol.* 1:263-264.
 41. Liebling, M., A.S. Forouhar, R. Wolleschensky, B. Zimmermann, R. Ankerhold, S.E. Fraser, M. Gharib, and M.E. Dickinson. 2006. Rapid three-dimensional imaging and analysis of the beating embryonic heart reveals functional changes during development. *Dev. Dyn.* 235:2940-2948.
 42. Bruneau, B.G. 2008. The developmental genetics of congenital heart disease. *Nature* 451:943-948.
 43. Bruneau, B.G., G. Nemer, J.P. Schmitt, F. Charron, L. Robitaille, S. Caron, D.A. Connor, M. Gessler, et al. 2001. A murine model of Holt-Oram syndrome defines roles of the T-box transcription factor Tbx5 in cardiogenesis and a disease. *Cell* 106:709-721.
 44. Zhu, Y., A.O. Gramolini, M.A. Walsh, Y.Q. Zhou, C. Sloach, M.K. Freidberg, J. Takech, H. Sun, et al. 2008. Tbx5-dependent pathway regulating diastolic function in congenital heart disease. *Proc. Natl. Acad. Sci. USA* 105:5519-5524.

Received 8 October 2007; accepted 26 November 2008.

Address correspondence to Karen Ocorr, Development and Aging Program, Neuroscience, Aging and Stem Cell Research Center, Burnham Institute for Medical Research, La Jolla, CA, 92037, USA. email: kocorr@burnham.org